A Highly Sensitive Square Wave Voltammetry Based Biosensor for Kinase Activity Measurements

Elza Snir, Einav Amit, Assaf Friedler, Shlomo Yitzchaik
Institute of Chemistry and the Center for Nanoscience and Nanotechnology, The Hebrew University of Jerusalem, Jerusalem 91904, Israel

Received 16 November 2014; revised 11 March 2015; accepted 30 March 2015
Published online 7 April 2015 in Wiley Online Library (wileyonlinelibrary.com). DOI 10.1002/bip.22653

ABSTRACT:

An electrochemical biosensor has been developed for ultrasensitive, label-free determination of protein kinase activity. The sensor is composed of a unique peptide monolayer on a gold electrode. It identifies the order change in the monolayer upon phosphorylation, via square wave voltametry (SWV) measurements. Disorder caused by the introduction of the phosphate groups onto the middle of the peptide sequence results in pinhole formation and therefore an increase in the electrochemical signal. The measured sensitivity was 100 nM of kinase and the dynamic range was 100 nM up to 11 μM. Sensitivity was an order of magnitude higher, and the dynamic range wider by two orders of magnitude, as compared to our previously reported impedimetric method, in which the sensitivity was 1 μM, and the dynamic range was 1–20 μM. © 2015 Wiley Periodicals, Inc. Biopolymers (Pept Sci) 104: 515–520, 2015.

Keywords: *peptide monolayer; kinase biosensor; electrochemistry*

Correspondence to: Shlomo Yitzchaik, Institute of chemistry and the center for nanoscience and nanotechnology, The Hebrew University of Jerusalem, Jerusalem 91904, Israel; e-mail: shlomo.yitzchaik@mail.huji.ac.il
Contract grant sponsor: SYMONE project (FET-UCOMP thematic area)
Contract grant number: FP7 318597
Contract grant sponsor: COST action (HINT)
Contract grant number: MP1202
Dedicated to: Prof. Dr. Luis Moroder, Max Planck Institut für Biochemie, Martinsried Germany

This article was originally published online as an accepted preprint. The "Published Online" date corresponds to the preprint version. You can request a copy of any preprints from the past two calendar years by emailing the Biopolymers editorial office at biopolymers@wiley.com.

INTRODUCTION

Protein kinase-catalysed phosphorylation plays a significant role in regulating signaling pathways in cells.[1] Protein function is regulated in many cases by transferring the phosphoryl group from the γ-position of adenosine triphosphate (ATP) to specific serine, threonine, or tyrosine residues of proteins.[2] Abnormal protein kinase activity results in malfunction of cellular signaling networks, creating cellular conditions that may facilitate cancer development[3] and other proliferative diseases.[4] The levels of many kinases are elevated in cancer.[5] Thus, developing ultrasensitive kinase sensors is highly important for cancer detection. It will also help in understanding the basic mechanism of action of kinases, and their partner proteins at the molecular level[6] and have applications in anticancer drug development.[7,8]

Nowadays, various methods were developed in order to detect protein phosphorylation. Proteomics is used to detect phosphorylated proteins and phosphorylation sites.[9,10] Flow cytometry uses antibodies to detect phosphorylation inside cells.[11] Many other methods use spectroscopic detection, with nanoparticles acting as markers.[12–15]

Electrochemistry is one of the promising strategies for profiling and characterizing enzymatic reactions due to its sensitivity, simplicity, and diversity. This has driven the development of many electrochemical enzymatic assays,[16–18] and specifically, kinase assays.[19–21] On the background of the diverse electrochemical methods, electrochemical impedance spectroscopy (EIS) has emerged as a powerful tool to study this interaction by detecting changes in capacitance and

interfacial electron transfer resistance (R_{CT}) at the electrode surface.[22,23] We have previously reported a very sensitive method for detection of kinase activity[24] based on this technique. We also showed that EIS is more efficient than ion-sensitive field effect transistor (ISFET) for kinase biosensing.[24]

In this system, a gold electrode is coated with a thiol containing peptide monolayer. The monolayer is then phosphorylated by incubation with a kinase enzyme, and undergoes conformational changes leading to a change in the electrochemical signal measured before and after phosphorylation.

The proposed mechanism of monolayer transformation as a result of phosphorylation is that the monolayer packing changes to a less organized peptide ensemble. In the preceding study, we showed that the electrostatic characteristics of the redox active species have little influence on the transduction of the electrochemical signal. In this system, pinhole creation in the ordered monolayer was found to be the dominant effect and not repulsion of the negatively charged redox species that are playing a dominant role in other EIS kinase sensors.[20,22] This was concluded after a drop in impedance was observed following phosphorylation, and pinhole formation was observed in AFM measurements. After dephosphorylation, impedance returned to its original value, and the pinholes disappeared. This conclusion was further supported by contact angle measurements that showed a reversible decrease and increase in contact angle after phosphorylation and dephosphorylation.

To validate that the peptide does not desorbs from the electrode following phosphorylation, several cycles of phosphorylation—dephosphorylation were preformed on the same monolayer. After two repetitive cycles of phosphorylation—dephosphorylation, the original impedance value was restored. We concluded that the phosphorylation was not destructive to the peptide monolayer.

In addition, monolayers containing alanine instead of serine at the phosphorylation site did not show significant change in impedance after incubation with kinase enzymes. This showed that the electrochemical signal changed as a result of phosphorylation and not from the destruction of the monolayer.

The peptide sequences were chosen for their ability to undergo intensive phosphorylation by protein kinases. This was done by scanning substrate peptide libraries for each kinase, by PepChip® microarray analysis.[25] On the earlier study we showed the enhanced sensitivity of these sequences to the corresponding kinases using an electrochemical signal received from EIS data. Peptide **1** (CGGGPPRRSSIRNAH) was synthesized as target for Protein Kinase C (PKC) and peptide **2** (CGGGLRRRLSDSSFI) as target for Protein Kinase A (PKA). These sequences are taken from the kinases recognition motif, with the phosphoryl serine in the middle of the sequence. This, according to our model (Figure 1), gives us enhancement of the electrochemical signal upon phosphorylation. The motifs were added tri–glycine spacers, in order to create greater packing density, and a terminal thiol—containing cysteine residue, as a linker to the gold surface. Overall, these two peptides exhibited very high degrees of phosphorylation, as evaluated from EIS. R_{CT} decreased from about 14 kΩ to 70 Ω in case of PKC mediated phosphorylation of peptide **1**, and to 150 Ω, in case of PKA mediated phosphorylation of peptide **2**.

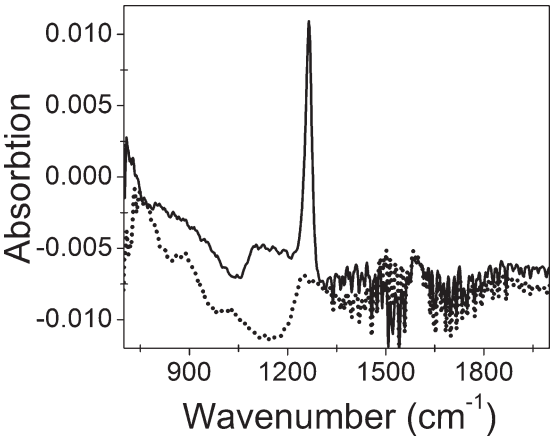

FIGURE 1 FTIR spectra of peptide **1**-coated gold-electrode before (dotted line) and after phosphorylation (solid line), by PKC.

In the current study, we investigated our system by means of SWV. While previously we have shown that the EIS can be used as an ultrasensitive method, we show here that the SWV technique is more rapid, accurate, and nondestructive. The presented method is a very simple but especially sensitive technique for the detection of kinase-mediated phosphorylation, without the need for the introduction of any other chemical labeling of the substrate or enzyme.[25] The method involves the creation of a unique peptide monolayer on gold electrodes, and measurements of SWV before and after the enzymatic phosphorylation reaction.

MATERIALS AND METHODES

Materials and Reagents

All chemicals, unless mentioned otherwise, were of analytical grade and were used as received. All aqueous solutions were made with triple-distilled water (TDW), 18.3 MΩ cm, purified with Barnsted Easypure UV system.

Phosphorylase enzymes: Purified, recombinant full-length PKA activity: 1665 nmol/mg/min, PKC activity: 1914 pmol/μg/min, supplied as GST fusion protein, and ATP were purchased from Cell Signaling Technology (CST), (Boston, USA).

AP, (10,000 U/ml) was purchased from New England Biolabs (ON Canada).

Peptide Synthesis and Purification

Peptide synthesis was done on a Liberty peptide synthesizer with a Discover single mode microwave module from CEM (NC), using standard Fmoc chemistry. Protected amino acids were purchased from Luxembourg Bio Technologies (Tel Aviv, Israel), Iris biotech GmbH (Marktredwitz, Germany), and Chem-Impex (Wood Dale, IL). Coupling of modified residues to the resin was performed with Fmoc-*N′*-Acetyl-L-lysine and Fmoc-*O*-benzyl-L-phospho-serine (Novabiochem). Following coupling of Phospho-serine, all fmoc deprotections were carried out without microwave heating. The peptides were purified on an ACE C8 semi-preparative column using gradients of 5–60% acetonitrile in water, with 0.1% trifluoroacetic acid (TFA) in both solvents. The identity of the peptides was validated using an Applied Biosystems Voyager-DE Pro MALDI TOF mass spectrometer and verified to be within ± 1 Da of the theoretical mass. The purity of all peptides was verified to be >95% for nonlabeled peptides and >90% for fluorescein-labeled peptides by analytical HPLC. The purified peptides were lyophilized from 30% acetic acid to remove residual TFA. The concentrations of the peptides were measured by UV absorbance at 280 nm using the extinction coefficient 5500 M^{-1} cm^{-1} for tryptophan.

Gold Electrodes Preparation

Polycrystalline bulk gold electrodes (CH instruments) with a surface area of 7.94 mm^2 were used for electrochemical measurements. These homemade electrodes were hand-polished on micro-cloth pads (CH instruments) with deagglomerated alumina suspension (Buehler, Lake Bluff, IL) of decreasing particle size (1.0 and 0.05 μm) using a homemade polisher. After being polished the electrodes were sonicated in TDW for 15 min followed by additional sonication in EtOH solution (50% v/v, Sigma Aldrich, Israel) for 10 min. Copiously washed gold electrodes were then cleaned with warm HNO_3 (70%) (Sigma Aldrich, Israel) during 20 min. The electrodes were then rinsed with TDW and cycled from -0.4 to 1.6 V in 0.5*M* H_2SO_4 (Sigma Aldrich, Israel) at 0.1 Vs^{-1} until a stable reproducible cyclic voltammogram were obtained-electrochemical reduction of an AuO monolayer.

Electrode Surface Modification

Treated gold macroelectrodes were immersed into prepared peptide solution (1.0 m*M*) and were kept for 16 h at 25°C. After removal, the electrodes were rinsed three times in TDW and dried under nitrogen gas stream. Electrochemical characterization was preformed directly after the electrodes were washed. For each peptide sequence several electrodes were prepared. Solution was prepared by dissolved of thiol-terminated peptide in weakly based TDW pH > 7.5.

Kinase Catalyzed Phosphorylation

Peptide modified gold electrodes were reacted with different kinases. Each kinase activity, for the same substrate, was examined simultaneously and separately for the three enzymes (PKA, PKC, and CaMK2). Kinase derived phosphorylation was carried out by dripping of kinase solution on modified electrodes surfaces at room ambient. Reaction medium (10,000 n*M* kinase in a final reaction volume of 100 μl) containing 20 m*M* Tris-HCl buffer solution (pH 7.5), 10 m*M* $MgCl_2$, 50 m*M* KCl, 5 m*M* β-glycerophosphate, 0.1 m*M* Na_3VO_4 (CST, Boston, MA) and 100 μM ATP. The reaction was initiated with the addition of the fresh prepared protein kinase solution and stopped by rinsing after 20 min. Electrodes were carefully washed multiple times using Tris buffer, followed by a brief sonication in TDW.

Phosphatase Catalyzed Dephosphorylation

Hydrolysis of surface grafted phosphorylated peptides was performed in the presence of AP, 0.1 Units in a final reaction volume of 100 μl, for 20 min at room ambient. One unit AP was dissolved in a 1 ml of tris borate buffer (Sigma Aldrich, Israel), (pH 8.5), containing 10 m*M* $MgCl_2$ (Sigma Aldrich, Israel). (One unit (U) is defined as the amount of enzyme that can hydrolyze 1 μmol of phosphorylated peptide in a total reaction volume of 1 ml in 1 min at 37°C). Electrochemical measurements were taken following each modification step.

Electrochemical Characterizations

CV, SWV, and EIS measurements were performed using an Autolab PGSTAT12 digital potentiostat (EcoChemie BV, Utrecht, The Netherlands) connected to NOVA software. A conventional three-electrode cell was employed, with a peptide modified gold electrode as working electrode, and a standard Ag/AgCl reference electrode (Metrohm) with a KCl concentration of 3.0*M*.

Cyclic Voltammetry (CV): The CV experiments were recorded by scanning the potential from -0.3 to 0.6V (vs. Ag/AgCl) and back, employing a scan rate of 10 mV/s. Prior to the scan, the electrode was kept at -0.3 V for 10 s. To provide redox species, a 1 m*M* $[Fe(CN)_6]^{3-}$ (Sigma Aldrich, Israel) solution additionally containing 100 m*M* KNO_3 as supporting electrolyte was used.

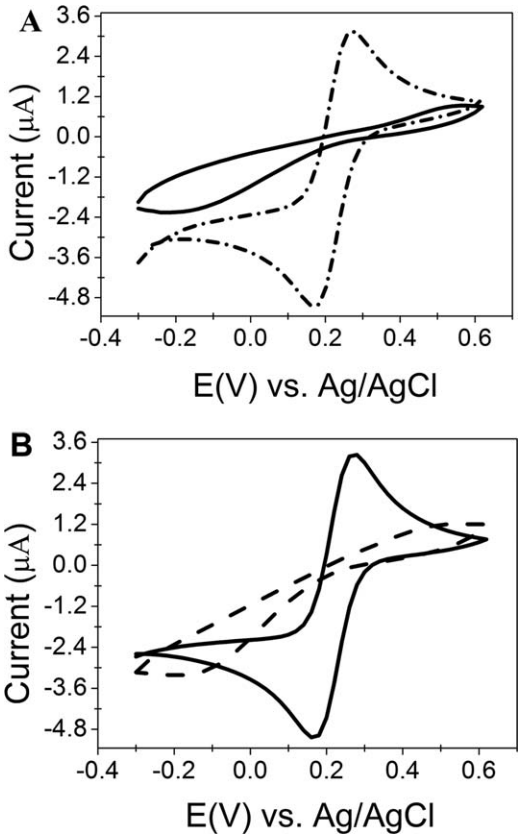

FIGURE 2 (A) Cyclic voltammograms of 1 m*M* $[Fe(CN)_6]^{3-}$ solution at two stages: before (•—•) and after peptide assembly (—) with an aqueous solution of 1.0 m*M* of peptide **2**. (B) After phosphorylation by PKA (—) and dephosphorylation by AP (---).

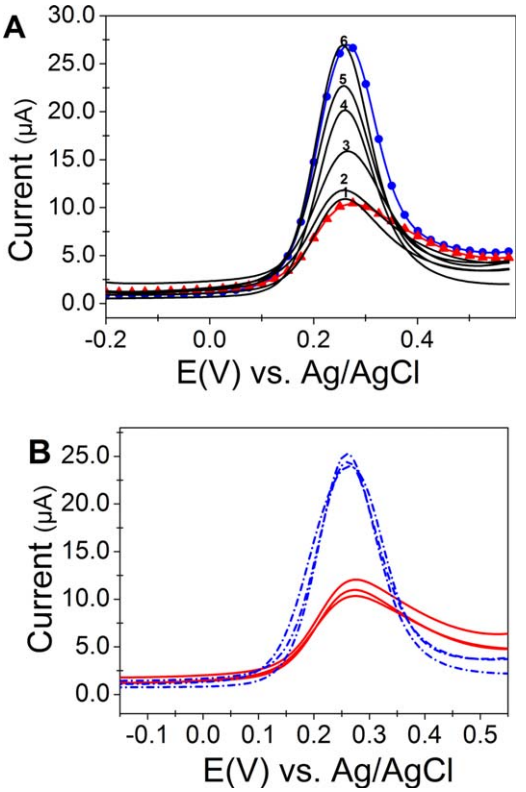

FIGURE 3 (A) Square wave voltammogram of 1 m*M* $[Fe(CN)_6]^{3-}$ obtained at the peptide **1**-modified gold electrode before (▲) and after (all others) the addition of 20,000 n*M* (6), 970 n*M* (5), 490 n*M* (4), 97 n*M* (3), 49 n*M* (2), and 10 n*M* (1) PKC for 20 min. Scatter-line curve shows the control experiment of bare gold electrode (•). (B) SWV voltammogram obtained at the substrate **1** peptide-modified three different gold electrodes, prepared under the same conditions, before (—) and after (•—•) the addition of 10 μ*M* PKC for 20 min.

Square wave voltammetry (SWV): These voltammograms were obtained by scanning from −0.3 to −0.6 V with a step potential of 25 mV, amplitude of 10 mV and frequency 25 Hz at a scan rate of 625 mV/s. The redox species solution was the same as in the CV experiments. In the current study the distance between working and counter electrodes was invariable.

Electrochemical impedance spectroscopy (EIS): The measurements solution contained 5.0 m*M* $K_3Fe(CN_6)$, 5.0 m*M* K4Fe(CN_6), and 0.1*M* of KCl (all from Sigma Aldrich, Israel) as supporting electrolyte. The spectra were recorded at a frequency range of 0.1 Hz–10 kHz with an amplitude of 10 mV, at the formal potential of the redox couple versus Ag/AgCl electrode.

Preparation of Gold Surfaces for FTIR Measurements

The measurements were done on gold surfaces (200 nm thick) on borosilicate (1.1 mm thick) with Cr adhesion layer (2.5 nm). The gold substrates were rinsed three times alternately in pure ethanol, acetone, and ultrapure water, and hydrogen flame annealed to achieve highly smooth surfaces yielding surface roughness of about 2 nm. The peptide monolayer assembly and phosphorylation were performed in the same manner as on the gold electrodes.

RESULTS AND DISCUSSION

To validate that the monolayer undergoes phosphorylation, FTIR studies were performed (see Figure 1). After phosphorylation, a distinct phosphate peak appears at 1260 cm^{-1}. Figure 2 shows the voltammetric response obtained from the oxidation scans after the self-assembling of peptide on the gold electrode following the PKA-catalyzed phosphorylation reaction.

The changes in the current response provided the quantitative information about the extent of phosphorylation reaction. Before phosphorylation the measured oxidation current was 1.3 μA, and after phosphorylation with PKA it was 3.3 μA.

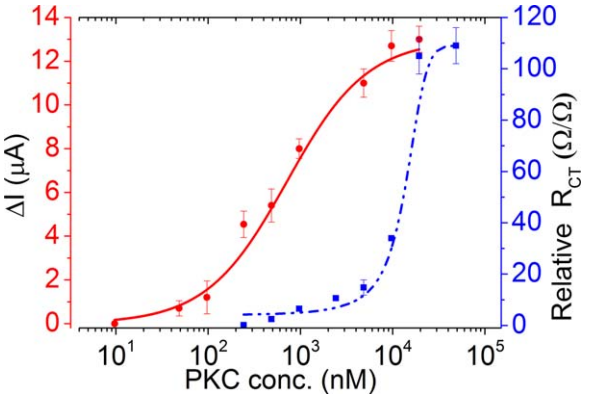

FIGURE 4 Dose response curve for increasing concentrations of PKC. Δ*I*, calculated from the SWV data, represents the current difference after and before phosphorylation of the peptide 1 monolayer. Relative R_{CT}, calculated from the EIS data, represents the resistance (R_{CT}) ratio before and after phosphorylation of the peptide 1 monolayer. Phosphorylation was performed in the presence of increasing concentrations of PKC. The error bars represent the error range calculated from three independent measurements.

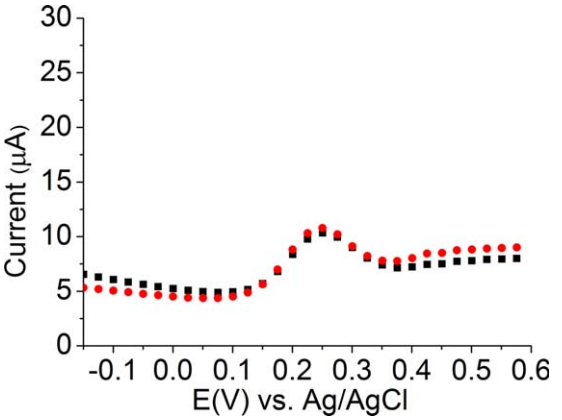

FIGURE 5 SWV voltammogram obtained at the peptide 3-modified electrodes, before (■) and after (•) the addition of 10 μ*M* PKC for 20 min.

After dephosphorylation with alkaline phosphatase (AP) the oxidation current returned to 1.7 μA.

For the optimization of experimental sensitivity, a series of measurements were taken in presence of varying PKC concentrations using the same assay conditions. The concentration dependence of the phosphorylation was determined by applying different kinase concentrations and measuring the current response. A saturation level in the signals was reached after using 20 μM PKC concentrations. When the reaction was carried out in presence of 30 μM kinase concentration, no significant increase in the reduction peak responses was recorded. The dependence of the current response on PKC concentration was recorded as shown in Figure 3.

Current difference (ΔI) and the relative charge transfer resistance (Relative $R_{CT} = R_{CT(\text{after phosphorylation})}/R_{CT\ (\text{before phosphorylation})}$) were measured and plotted in response to the varying concentrations of PKC on **1**-modified gold electrodes (Figure 4). The resulting dose–response curves are sigmoid-shaped. The lowest detectable concentration by SWV is 100 nM and a dynamic range from 100 nM up to 11 μM, with signal current range of 2–13 μA. In contrast, the lowest detectable concentration in the impedimetric method was 1 μM

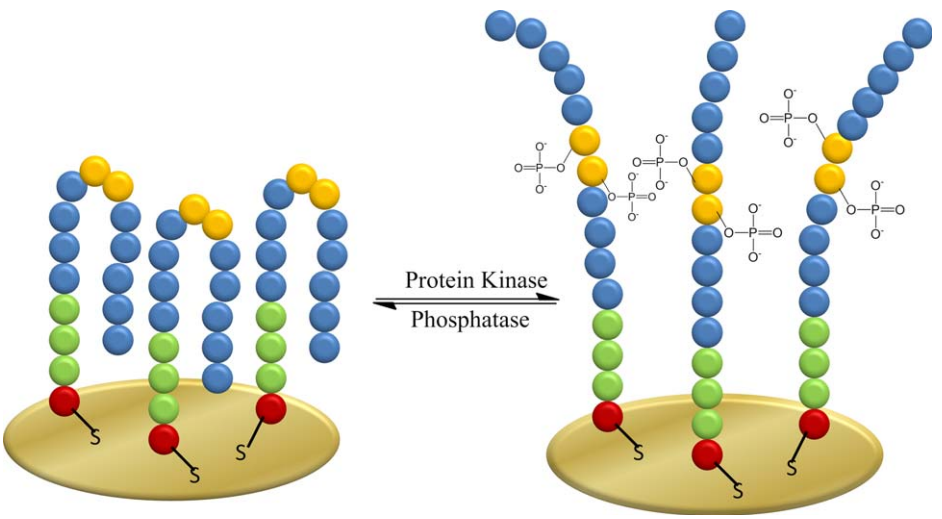

SCHEME 1 The suggested manner of the monolayer transformation before and after phosphorylation. The peptides are ordered in a dense monolayer, blocking the redox species from reaching the electrode. After phosphorylation, repulsion between the phosphate groups causes disruption in the order, thus leading to pinhole formation, and low impedance. Removal of the phosphate groups gives back the former ordered monolayer.

(relative $R_{CT} = 2.5$), and a dynamic range of 1–20 μM (relative R_{CT} from 2.5 ± 1 to 111 ± 7, respectively).

The reported sensitivity (100 n$M \cong 2 \times 10^{-2}$ Unit/ml) is improved compared with other reported kinase sensors[12,13,20,26–28] although other systems have shown better sensitivity,[14,21] which might be due to different reaction conditions–higher temperature and longer incubation time. The relatively high sensitivity is related to the density of the prephosphorylated monolayer, as observed by its impedance of around 10 kΩ, as compared with a few hundred ohms in other reported works.[20,22] After phosphorylation, the observed change in impedance was of several orders of magnitude, to a few hundred Ohms. This prominent change in the monolayer characteristics (Scheme 1) also affects the SWV measurements, as observed by the high oxidation currents received after phosphorylation.

To test the selectivity of the assay, we performed the same phosphorylation process with PKC using a peptide monolayer of Peptide **3** (CGGGHRSPRASPINR)—a peptide containing the linker and tri glycine spacer, but with a scrambled sequence of peptide **1**. As seen in Figure 5 we observed nearly no change in the current (10.0 ± 0.2 μA) before and after the incubation with PKC, showing that the phosphorylation was negligible.

CONCLUSIONS

The SWV method presented herein improves the kinase activity detection by an order of magnitude leading to detection in the nanomolar range, as compared to the previously reported impedimetric method and a dynamic range improvement of two orders of magnitude. SWV detection method is responsible for the improved performance of the biosensor since the surface chemistry is identical for the EIS measurements. We assume that the pinhole amplification mechanism may contribute more to the enhanced sensitivity. Such improvement, combined with rapid measurement time and simplicity of results interpretation, we conclude that the SWV method is superior to the previously reported impedimetric method. This method can be employed in the future for diagnostic, when calibrated for a specific kinase and for other drug development purposes.

REFERENCES

1. Hunter, T. Cell 2000, 100, 113–127.
2. Cohen, P. Nat Rev Drug Discov 2002, 1, 309–315.
3. Fabbro, D.; Cowan-Jacob, S. W.; Möbitz, H.; Martiny-Baron, G. Methods Mol Biol 2012, 795, 1–34.
4. Shimizu, T.; Usuda, N.; Sugenoya, A.; Masuda, H.; Hagiwara, M.; Hidaka, H.; Nagata, T.; Iida, F. Cell Mol Biol 1991, 37, 813–821.
5. Robertson, J. F.; O'Neill, K. L.; Thomas, M. W.; McKenna, P. G.; Blamey, R. W. Br J Cancer 1990, 62, 663–667.
6. Martić, S.; Beheshti, S.; Kraatz, H. B.; Litchfield, D. W. Chem Biodivers 2012, 9, 1693–1702.
7. King, S. I.; Purdie, C. A.; Bray, S. E.; Quinlan, P. R.; Jordan, L. B.; Thompson, A. M.; Meek, D. W. Breast Cancer Res 2012, 14, R40.
8. Lipchik, A. M.; Parker, L. L. Anal Chem 2013, 85, 2582–2588.
9. Mann, M.; Ong, S. E.; Grønborg, M.; Steen, H.; Jensen, O. N.; Pandey, A. Trends Biotechnol 2002, 20, 261–268.
10. Molina, H.; Horn, D. M.; Tang, N.; Mathivanan, S.; Pandey, A. Proc Natl Acad Sci U S A 2007, 104, 2199–2204.
11. Zell, T.; Khoruts, A.; Ingulli, E.; Bonnevier, J. L.; Mueller, D. L.; Jenkins, M. K. Proc Natl Acad Sci U S A 2001, 98, 10805–10810.
12. Gupta, S.; Andresen, H.; Ghadiali, J. E.; Stevens, M. M. Small 2010, 6, 1509–1513.
13. Anderson, J. C.; Peck, S. C. Plant J 2008, 55, 881–885.
14. Chen, Z.; He, X.; Wang, Y.; Wang, K.; Du, Y.; Yan, G. Biosensors Bioelectron 2013, 41, 519–525.
15. Shachaf, C. M.; Elchuri, S. V.; Koh, A. L.; Zhu, J.; Nguyen, L. N.; Mitchell, D. J.; Zhang, J.; Swartz, K. B.; Sun, L.; Chan, S.; Sinclair, R.; Nolan, G. P. PLoS One 2009, 4, e5206.
16. Langer, J. J.; Filipiak, M.; Ke˛cińska, J. M.; Jasnowska, J.; Włodarczak, J.; Buładowski, B. Surf Sci 2004, 573, 140–145.
17. Rahman, M. M.; Shiddiky, M. J. A.; Rahman, M. A.; Shim, Y.-B. Anal Biochem 2009, 384, 159–165.
18. Wei, M.-Y.; Famouri, P.; Guo, L.-H. TrAC Trends Anal Chem 2012, 39, 130–148.
19. Song, H.; Kerman, K.; Kraatz, H. B. Chem Commun (Cambridge) 2008, 4, 502–504.
20. Wilner, O. I.; Guidotti, C.; Wieckowska, A.; Gill, R.; Willner, I. Chemistry 2008, 14, 7774–7781.
21. Wang, J.; Shen, M.; Cao, Y.; Li, G. Biosens Bioelectron 2010, 26, 638–642.
22. Martić, S.; Labib, M.; Kraatz, H. B. Analyst 2011, 136, 107–112.
23. Esseghaier, C.; Bergaoui, Y.; ben Fredj, H.; Tlili, A.; Helali, S.; Ameur, S.; Abdelghani, A. Sensors Actuat B: Chem 2008, 134, 112–116.
24. Snir, E.; Joore, J.; Timmerman, P.; Yitzchaik, S. Langmuir 2011, 27, 11212–11221.
25. Diks, S. H.; Kok, K.; O'Toole, T.; Hommes, D. W.; van Dijken, P.; Joore, J.; Peppelenbosch, M. P. J Biol Chem 2004, 279, 49206–49213.
26. Xu, X.; Nie, Z.; Chen, J.; Fu, Y.; Li, W.; Shen, Q.; Yao, S. Chem Commun (Camb) 2009, 45, 6946–6948.
27. Ji, H.; Yang, Y.; Liu, H.; Chen, J. K.; Liu, B. Chem Commun (Camb) 2009, 12, 1508–1510.
28. Miao, P.; Ning, L.; Li, X.; Li, P.; Li, G. Bioconjug Chem 2012, 23, 141–145.